S0013-4651(98)01-017-9 CCC: $7.00 

# Glass-to-Glass Bonding for Vacuum Packaging of Field Emission Display in an Ultra-High-Vacuum Chamber Using Silicon Thin Film

**W. B. Choi,[a,z] B. K. Ju,[a] Y. H. Lee,[a] S. J. Jeong,[b] N. Y. Lee,[b] M. Y. Sung,[c] and M. H. Oh[a]**

[a]*Electronic Materials and Devices Research Center, Korea Institute of Science and Technology, Seoul 130-650, Korea*
[b]*Information Display Research Institute, Orion Electric Company, Suwon, Korea*
[c]*Department of Electrical Engineering, Korea University, Seoul, Korea*

Field emission displays (FEDs) are among the most promising flat panel displays, and require a high vacuum for long-term performance and reliability. In this paper, glass-to-glass electrostatic bonding is presented for providing an in situ vacuum packaging of an FED panel in an ultra-high-vacuum chamber, based on a conventional Si-to-glass anodic bonding mechanism. Using radio-frequency sputter deposition, amorphous silicon films have been formed on Sn-doped $In_2O_3$ coated glass substrates. Secondary ion mass spectroscopy was used to characterize the kinetics of the glass-to-glass electrostatic bonding. In order to investigate the applicability of this bonding technique to the in situ vacuum packaging of FED devices, the hermetic sealing test of FED panels with an exhausting hole sealed by this technique was experimented under $10^{-8}$ Torr vacuum level. This technique is suitable for mass production environments since it is capable of high-speed sealing and eliminating the outgassing problem.


Manuscript submitted January 9, 1998; revised manuscript received September 8, 1998.

Field emission display (FED) devices require significantly high vacuum for providing long-term performance and ensuring reliability.[1,2] The vacuum level must be held to $10^{-8}$ Torr for the stable operation of FED devices. The vacuum packaging of FED devices is currently performed in a manner analogous to a cathode ray tube (CRT). The FED panel is put on a vacuum system, which is sealed to an exhausting tube on the panel. The FED panel is then brought slowly up to 350°C under high vacuum and baked for several hours to eliminate all contaminated gasses. Once the requisite vacuum level is obtained, the FED panel is cooled to the room temperature, and the exhausting tube is heated until it collapses and seals off the FED device. The pumping procedure of an FED panel must be considered in order to overcome effects which reduce the vacuum level in the panel. The microstructure configuration of an FED panel imposes a constraint on feeding molecular gases to the pumping source. If a pumping system is capable of maintaining a vacuum of $10^{-8}$ Torr or better, the vacuum level of an FED panel at a location of a few centimeters away from the system could be $10^{-5}$ Torr or worse.[3] Moreover, the vacuum of an FED panel could be seriously affected by the outgassing effect inside the exhausting tube, when the exhausting tube was heated and melted to seal off the panel.

The elimination of the exhausting tube from an FED panel can lead to an increase in the vacuum conductance during the pumping procedure, overcoming the outgassing problem during the sealing-off process and thinning the thickness of the FED panel.

It may be possible to realize an ideal hermetic seal package of an FED panel without using the exhausting tube, if a solid-state bonding technique can be performed between the glass substrates. Many bonding techniques have been developed recently, e.g., silicon direct bonding,[4,5] anodic bonding,[6-10] and eutectic bonding.[11,12] Especially, the anodic bonding technique has been widely employed in microsensors and micromechanical devices due to the relatively low temperature requirement, its simple process, and high hermetic sealing capability.[13-15] Various processes have been developed for the silicon-to-bulk glass bonding and the silicon-to-silicon bonding using the deposited glass layer.[16-18]

In this work, since the anodic bonding technology can be used to realize an ideal hermetic seal package, this technology is applied to the glass substrate and carried out developing the glass-to-glass bonding technique. In this bonding method, the most significant feature is the use of silicon film compared to the conventional anodic bonding process using glass film. The bonding occurs at the interface between the silicon film and the glass substrate. Furthermore, a new vacuum packaging method for an FED panel is developed, which can eliminate the exhausting tube and shorten the pumping time by using the glass-to-glass bonding technology.

[z] E-mail: cwb@kistmail.kist.re.kr

## Experimental

Amorphous silicon thin film was deposited by a radio-frequency (rf) magnetron sputtering at the substrate temperature of 120°C on the front glass substrate coated with a transparent electrode Sn-doped $In_2O_3$ (ITO) layer, which has a sheet resistance of about 80 Ω/□. The 3 in. silicon disk target with 99.999% purity was used. The base pressure in the chamber was adjusted to $2 \times 10^{-5}$ Torr, and the pressure during the deposition was maintained at $4 \times 10^{-3}$ Torr. The sputtering was carried out in 100% argon gas and the target rf power density was 2.2 W/cm$^2$. Soda-lime glass substrates are preferred as a base plate in FED devices for its vacuum sealing property such as permeation, which is the transfer of gas from the high pressure to the low pressure side. The most significant problem stems from the helium permeation through the glass substrate. It is known that the helium partial pressure increases from a base pressure of $10^{-16}$ Torr to $10^{-6}$ Torr in three days for silica, one month for Pyrex glass and 100 years for soda-lime glass.[19] In these experiments, Corning no. 0080 glass (soda-lime glass, coefficient of thermal expansion: $92.5 \times 10^{-7}$ cm/°C) coated with the ITO was used as the base plate. Its main features of the chemical and physical properties are summarized in Table I. In the anodic bonding process, since the surface morphology was one of the most critical bonding parameters, an atomic force microscope (AFM) was adopted to examine the surface roughness of the bare glass, ITO layer and silicon film.

For the bonding procedure, a typical anodic bonding method was used (Fig. 1), wherein the ITO layers served as the electrode. At an elevated temperature, an electrostatic voltage was applied across the ITO layers so that the glass substrate was at a negative voltage with respect to the silicon film. The parameters investigated during the bonding process were the bonding temperature and applied voltage.

A 4 in. FED panel was fabricated to examine the hermetic sealing capability of the glass-to-glass bonding. The glass paste was dispensed on a cleaned anode glass substrate in $9 \times 6$ cm square pattern and heated at 380°C in order to preglaze the glass paste. Then, a cathode glass substrate was put on the pasted anode glass substrate and heated to 415°C to melt the glass paste. Both the exhausting tube and hole were formed on the panel to perform the hermetic sealing test. A silicon layer was deposited around the exhausting hole of the FED panel, which was then sealed by the glass-to-glass bonding process.

## Results and Discussion

The increase in the surface roughness decreases the bonding strength and it may even cause the bonding to fail. Figure 2 shows

S0013-4651(98)01-017-9 CCC: $7.00 

**Table I. Comparison of chemical and physical properties of the materials that were used.**

| Properties \ Materials | No. 0080 Soda-lime glass | No. 7740 Pyrex glass | No. 7059 Pyrex glass |
|---|---|---|---|
| Composition (%) | | | |
| $SiO_2$ | 73.2 | 80.8 | 49 |
| $Na_2O$ | 16.8 | 4.2 | 0.07 |
| $Al_2O_3$ | 1.4 | 2.2 | 10 |
| $K_2O$ | 0.3 | | |
| $B_2O_3$ | | 12.8 | 15 |
| PbO | | | |
| RO | | | 25 |
| BaO, MgO, CaO | 8.2 | | 0.93 |
| Viscosity-thermal properties (°C) | | | |
| Strain point | 470 | 510 | 593 |
| Annealing point | 510 | 560 | 639 |
| Softening point | 695 | 821 | 844 |
| Coefficient of thermal expansion ($\times 10^{-7}$ cm/°C) | 92.5 | 32.5 | 45.6 |

the AFM images of the bare glass substrate, ITO layer, and silicon layer. From the AFM results, it was revealed that the roughness of the glass substrate coated with the ITO was slightly increased. Similar results were found for the silicon layer. The surface roughness of the silicon layer was within 20 nm peak-to-valley. Table II lists the surface roughness parameters of those AFM images.

In the anodic bonding process, temperature plays a crucial role since it increases the mobility of metal ions in the glass substrate. With raising the temperature of the glass, the metal ions become quite mobile and can be transferred by an applied electrical field. When an external voltage is applied across the electrodes, the space charge region is rapidly built at the interface between the silicon and the glass substrate. Most potential drop occurs in this region. In this case, the silicon and the glass substrate act as a parallel capacitor. The resulting large electrostatic force pulls the negative oxygen ions in the glass substrate from the bulk region to the surface region and forms Si–O–Si bonds originating either from the silicon oxidation at the interface or by the thermodehydration of the silicon-glass ensemble. The formation of a $SiO_2$ layer between the silicon and glass during the bonding process was proved by backscattering spectroscopy.[20]

Figure 3 shows the current-time characteristics measured during the bonding process. The current profile appears in accordance with the typical current-time curve for the anodic bonding. The higher the temperature was raised, the higher peak current was measured. Similar current-time characteristics were observed for the process with the voltage as the parameter, as displayed in Fig. 3b.

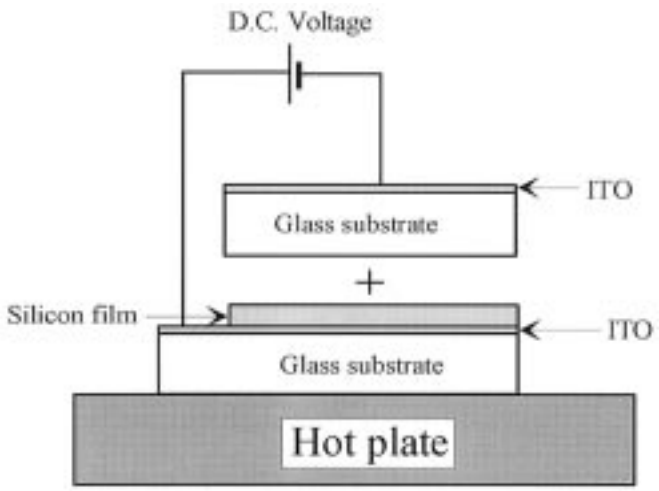


**Figure 1.** Schematic diagram of glass-to-glass bonding equipment.

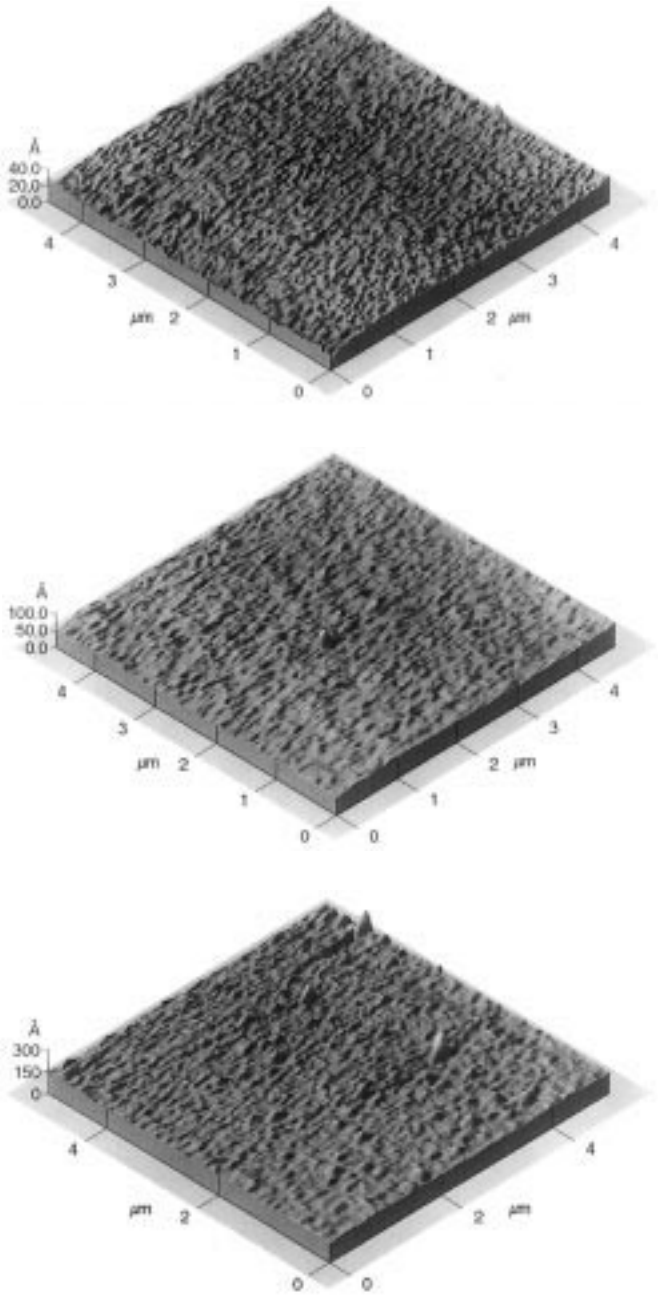


**Figure 2.** AFM images of the surface morphology: (a) bare glass substrate; (b) ITO layer; (c) silicon layer deposited by rf magnetron sputtering.

**Table II. Roughness parameters of AFM images for bare glass substrate, ITO layer, and silicon layer. (Unit: Å)**

| Roughness \ Substrate | No. 0080 bare glass substrate | ITO/No. 0080 | Si/ITO/No. 0080 |
|---|---|---|---|
| Mean height | 15 | 20 | 44 |
| Peak-to-valley | 34 | 82 | 196 |
| RMS roughness | 2.4 | 3.7 | 10 |
| Average roughness | 1.9 | 2.8 | 6.2 |

S0013-4651(98)01-017-9 CCC: $7.00 

The bonded samples were cut to investigate the bonded interface region of the glass-to-glass assembly. Figure 4 shows the cross-sectional photographs of a scanning electron microscope (SEM). When the pull tests were performed to measure the tensile strength, fracturing was seen at the bulk region of the glass substrate or the interface region between a silicon layer and an ITO layer on which the silicon layer was deposited. In case of fracturing at the interface, the silicon layer was removed from the glass substrate on which it was originally deposited and found on the glass substrate to be bonded. To examine both the migration of positive metal ions and negative oxygen ions in the glass substrate during the bonding process, secondary ion mass spectroscopy (SIMS) analysis was performed on both the bare glass substrate to be bonded before the process and the specimen fractured at the interface from the silicon layer to the glass substrate after the process (Fig. 5). The SIMS data were obtained by using the cesium ion ($Cs^+$) incident on the specimen to cause positive and negative secondary ions to be ejected. From the SIMS data, the residual thin ITO layer was observed at the front surface of the glass substrate to be bonded, as shown in Fig. 5a. From the spectra of Fig. 5b, it was apparent that the metal (Na, Al, K, Mg, and Ca) ions were almost depleted from the surface region of the glass substrate in contact with the silicon layer. It was also found that the residual indium and tin on the glass surface diffused in the silicon layer. From the negative SIMS analysis, it was easily observed that the significant feature was formed at $SiO_2$ depth profile of the surface region. This is in agreement with the usual anodic bonding mechanism where the metal ions are depleted from the surface of the glass substrate by the applied voltage and the resulting large electrostatic force pulls two glass substrates into intimate contact, thereby allowing the formation of atomic bonds.

In order to investigate the hermetic sealing probability of the exhausting hole sealed by the glass-to-glass bonding, the glass substrate and the FED panel with both the exhausting hole and tube were bonded at a temperature of 280°C with an electrostatic voltage of 300 $V_{DC}$ (Fig. 6). The FED panel sealed by the glass substrate was then put on a vacuum system, which was sealed to the exhausting tube on the panel (Fig. 7). During the pump-out process for one week,

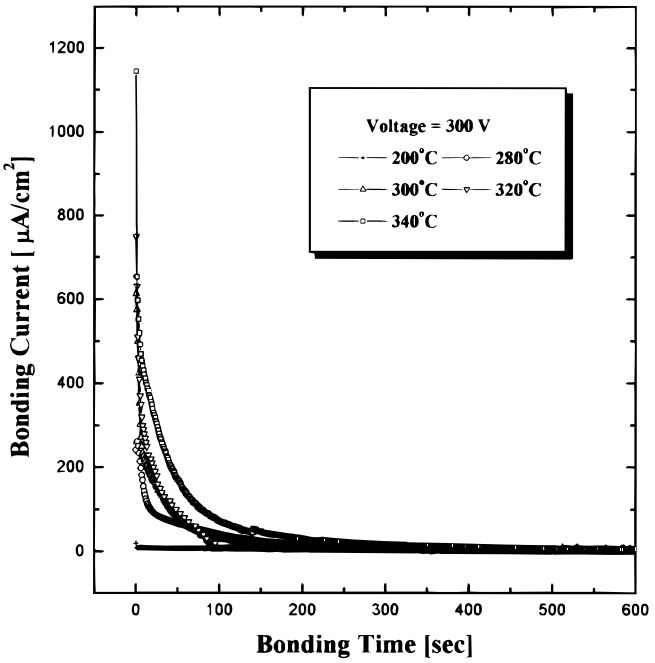


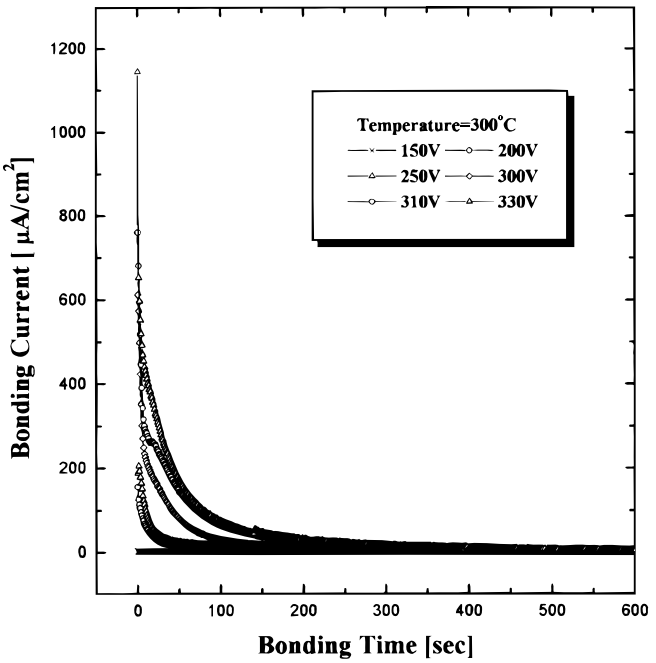


**Figure 3.** Typical current vs. time relationship during the bonding process as function of parameters (a) temperature; (b) applied voltage.

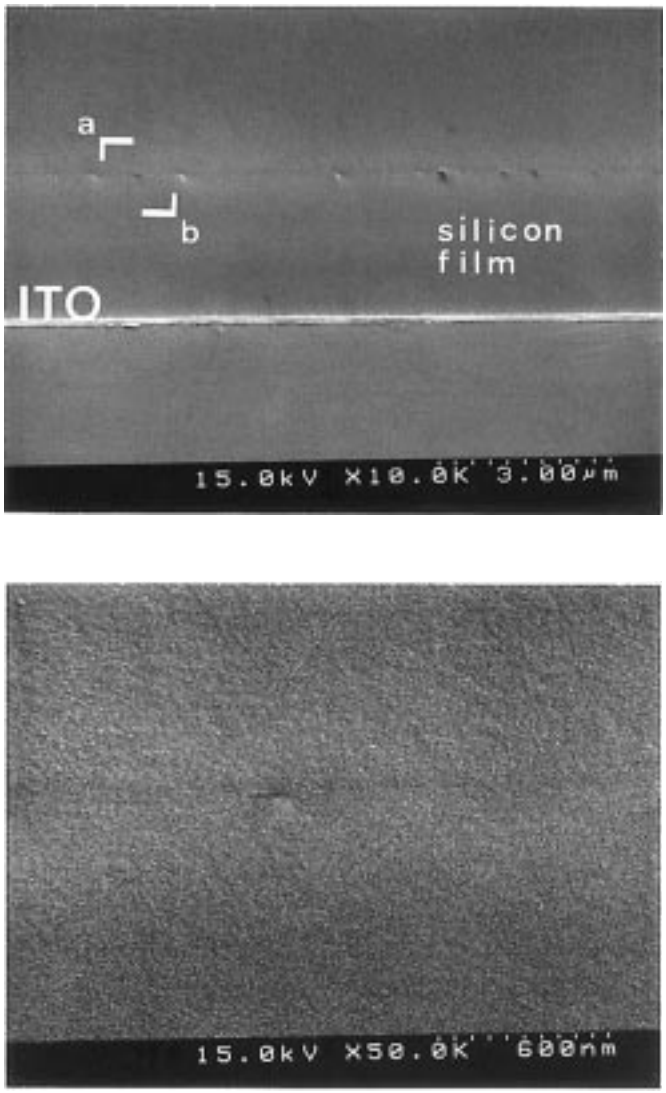


**Figure 4.** Cross-sectional SEM images: (a) bonded interface region of glass-to-glass ensemble; (b) region a-b.

S0013-4651(98)01-017-9 CCC: $7.00 

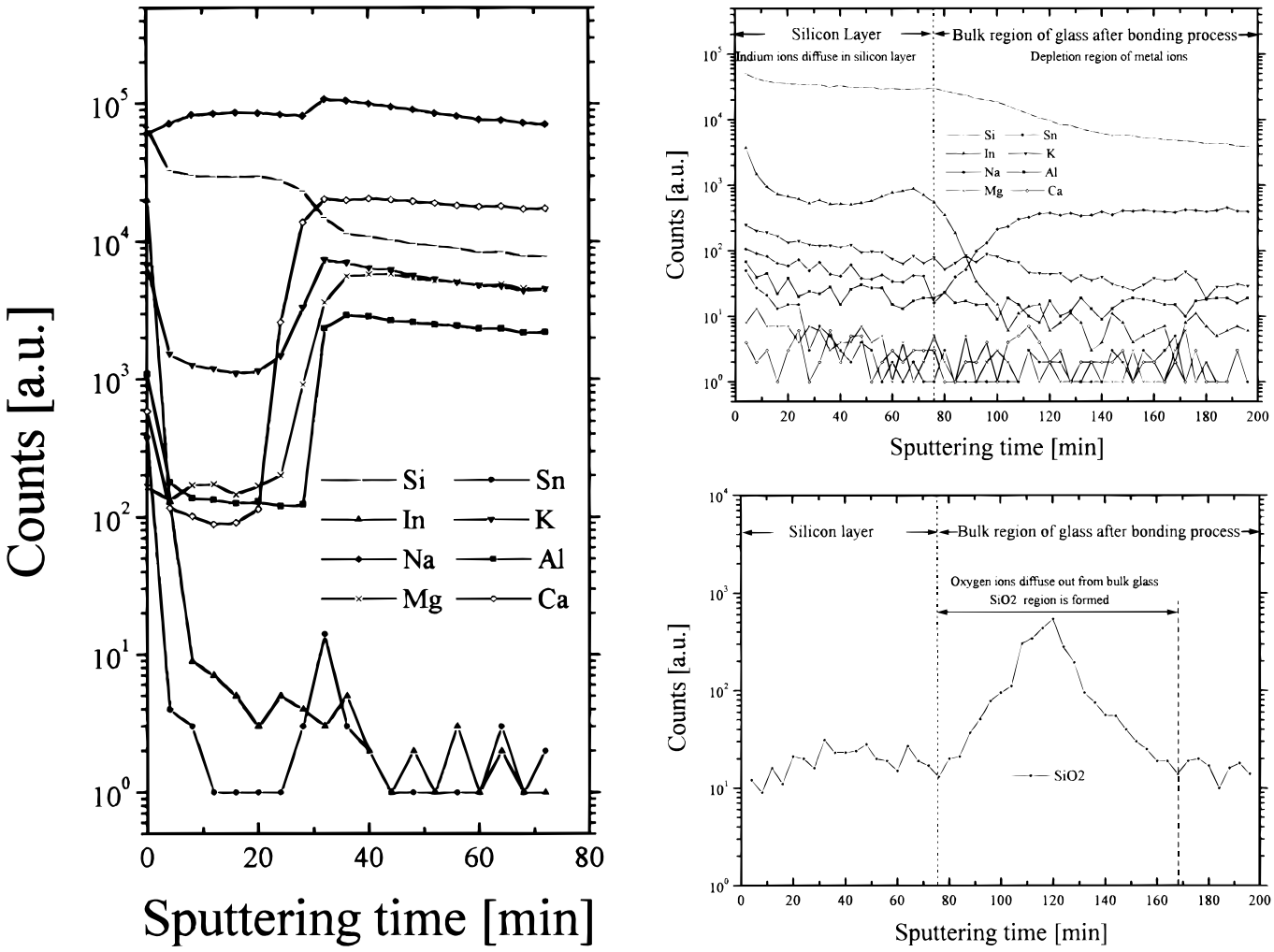


**Figure 5.** SIMS spectra: (a, left) positive analysis of the bare glass substrate to be bonded before bonding; (b, top right) positive analysis of the silicon film-glass substrate after bonding; (c, bottom right) negative analysis of the silicon film-glass substrate after bonding.

the change in the vacuum level in the buffer chamber was detected by an ion gauge. It was revealed that the panel maintained $2.2 \times 10^{-8}$ Torr vacuum level, as shown in Fig. 8. These results show that there is no leakage through the glass-to-glass bonding interface.

## Conclusion

A glass-to-glass bonding was performed using the silicon thin film deposited by rf magnetron sputtering, based on the conventional anodic bonding process. From the positive and negative SIMS analysis, it was confirmed that the metal and oxygen ions migrate in the glass substrate during the bonding process. This illustrates that the glass-to-glass bonding method using the silicon thin film follows the typical anodic bonding mechanism.

The applicability of this bonding method to the vacuum package of an FED panel was evaluated by the hermetic sealing test of the

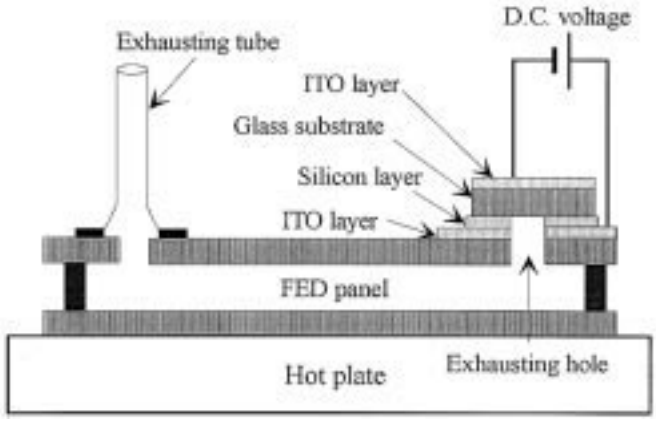


**Figure 6.** Schematic experimental setup for sealing of the exhausting hole.

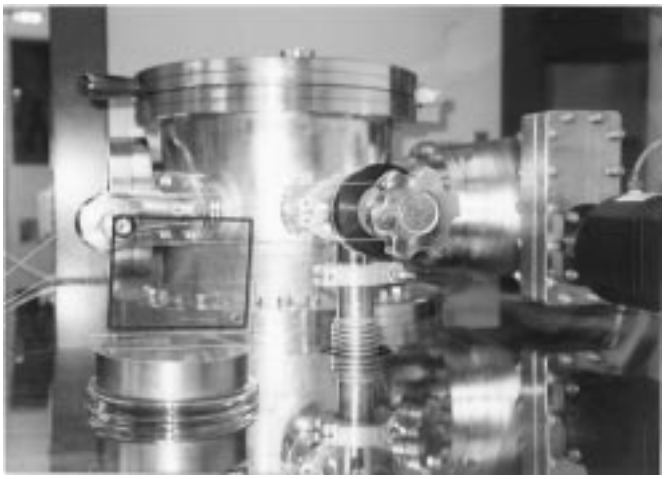

**Figure 7.** Hermetic sealing test of an FED panel with an exhausting hole sealed by glass-to-glass bonding.

S0013-4651(98)01-017-9 CCC: $7.00 

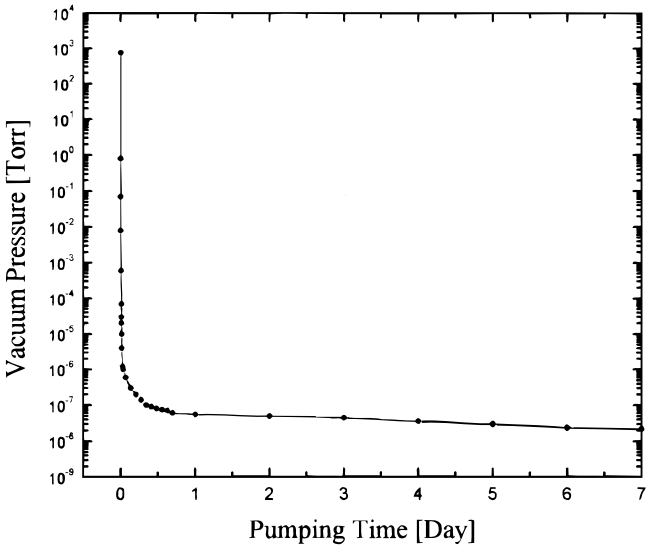


**Figure 8.** Leak test results of an FED panel during one week.

FED panel with an exhausting hole sealed by this technique. The FED panel was found to maintain $10^{-8}$ Torr vacuum level.

A packaging process using the glass-to-glass bonding method may be performed in an ultra-high-vacuum chamber, as shown in Fig. 9. This packaging method can eliminate the exhausting tube to minimize the thickness of FED panels while maximizing the throughput with high-speed sealing. Figure 10 shows the schematic final structure of an FED panel sealed using the proposed vacuum packaging method.

## Acknowledgments

The authors would like to thank Dr. Byungwhan Kim with the Center for Information and Communications at Korea University and Taeik Kim at the University of Washington for their continuous help and useful discussions in preparing this manuscript. This research was supported by the Korean Ministry of Trade, Industry and Energy.

*Korea Instituteof Science and Technology assisted in meeting the publication costs of this article.*

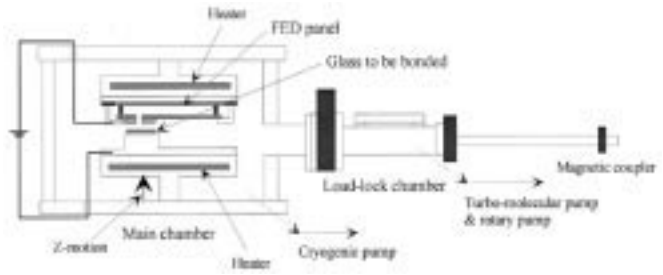


**Figure 9.** Schematic diagram of an in situ vacuum packaging system with load-lock chamber.

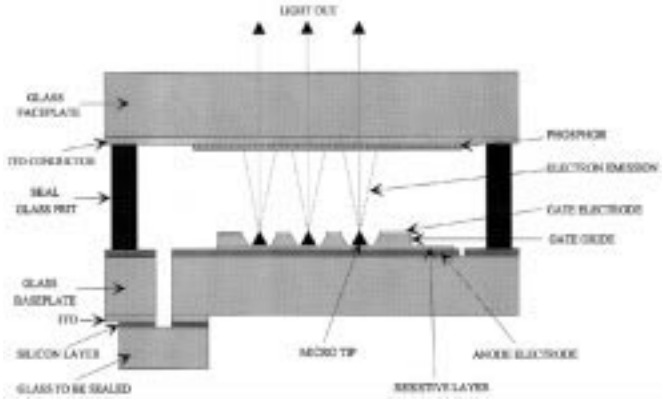


**Figure 10.** Diagram of tubeless vacuum packaged FED panel using glass-to-glass bonding.

## References

1. P. H. Holloway, J. Sebastain, T. Trottier, H. Swartand, and R. O. Petersen, *Solid State Technol.*, 47 (Aug 1995).
2. L. Branst, and F. Pothoven, *Semicond. Int.*, 109 (Jan 1996).
3. B. Gnade and J. Levine, *SID Seminar Lecture Note*, **1**, M-8/3 (1995).
4. W. P. Maszara, *J. Electrochem. Soc.*, **138**, 341 (1991).
5. B. K. Ju, Y. H. Lee, K. H. Tchah, and M. H. Oh, *J. Electrochem. Soc.*, **142**, 547 (1995).
6. B. Puers, E. Peeters, A. Bossche, and W. Sansen, *Sens. Actuators, A*, **21-23**, 108 (1990).
7. J. Berenschot, J. Gradeniers, T. Lammerink, and M. Elwenspoek, *Sens. Actuators, A*, **41-42**, 338 (1994).
8. D. Hurd, R. Caretta, and W. Gerberich, *J. Mater. Res.*, **10**, 337 (1995).
9. T. R. Anthony, *J. Appl. Phys.*, **54**, 2419 (1983).
10. A. Hanneborg and P. Øhlcker, *Sens. Actuators, A*, **21-23**, 151 (1990).
11. R. F. Wolffenbuttel, *Sens. Actuators, A*, **62,** 680 (1997).
12. S. E. Shoal and A. D. Feinerman, *J. Vac. Sci. Technol., A*, **12**, 19 (1994).
13. A. Hanneborg, S. Mack, and P. Øhlcker, *J. Micromech. Microeng.*, **1**, 139 (1991).
14. H. Baumann, S. Mack, and H. Münzel, in *Semiconductor Wafer Bonding: Physics and Applications*, C. E. Hunt, H. Baumgart, S. S. Iyer, T. Abe, and U. Gosele, Editors, PV 95-7, p. 471, The Electrochemical Society Proceedings Series, Pennington, NJ (1995).
15. B. Ziaie, J. Von Arx, R. Dokmeci, and K. Najafi, *J. Microelectromech. Sys.*, **5**, 166 (1996).
16. G. Wallis and D. I. Pomerantz, *J. Appl. Phys.*, **40**, 3946 (1969).
17. A. A. Brooks and R. P. Donovan, *J. Electrochem. Soc.*, **119**, 545 (1972).
18. Y. Kanda, K. Matsuda, C. Murayama, and J. Sugaya, *Sens. Actuators, A*, **21-23**, 939 (1990).
19. J. F. O'Hanlon, *A User's Guide to Vacuum Technology*, John Wiley & Sons, p. 170 (1989).
20. J. B. Lasky, S. R. Stiffer, F. R. White, and J. R. Abernathy, *Tech. Dig., Int. Electron Devices Meet.*, **28**, 684 (1985).